Chinese Journal of Chemical Engineering 58 (2023) 224–233

Contents lists available at ScienceDirect

Chinese Journal of Chemical Engineering

journal homepage: www.elsevier.com/locate/CJChE

Full Length Article

Solubility measurement, correlation and thermodynamic properties of 2,3,4-trichloro-1,5-dinitrobenzene in fifteen mono-solvents at temperatures from 278.15 to 323.15 K

Yun-Zhang Liu [1], Lu-Yao Zhang [2], Dan He [2], Li-Zhen Chen [1], Zi-Shuai Xu [2], Jian-Long Wang [1,*]

[1] School of Chemical Engineering and Technology, North University of China, Taiyuan 030051, China
[2] Gansu Yinguang Chemical Industry Group Co. Ltd, Baiyin 730900, China

ARTICLE INFO

Article history:
Received 9 May 2022
Received in revised form 17 October 2022
Accepted 20 October 2022
Available online 5 December 2022

Keywords:
2,3,4-Trichloro-1,5-dinitrobenzene (TCDNB)
Solid-liquid equilibrium
Laser dynamic method
Solubility model
Thermodynamics properties

ABSTRACT

The solubility of 2,3,4-trichloro-1,5-dinitrobenzene (TCDNB) was measured by a laser dynamic method over the temperature range from 278.15 K to 323.15 K under 0.1 MPa in fifteen mono-solvents (methanol, ethanol, isopropanol, *n*-butanol, toluene, dichloromethane, chloroform, tetrachloromethane, 1,2-dichloroethane, acetone, ethyl acetate, acetonitrile, *N*-methylpyrrolidone (NMP), *N,N*-dimethylformamide dimethyl sulfoxide (DMF), dimethyl sulfoxide (DMSO). The solubility of TCDNB could be increased with increasing temperature in fifteen mono-solvents. TCDNB solubility is in the following order at 298.15 K: NMP>DMF>DMSO>toluene>acetone>ethyl acetate>dichloromethane>1,2-dichloroethane>chloroform>acetonitrile>tetrachloromethane>methanol>ethanol>*n*-butanol>isopropanol.
The KAT-LSER model was used to investigate the solvent effect, which revealed that the hydrogen bond acidity of solvents has a greater effect on TCDNB solubility. The van't Hoff model, the modified Apelblat model, the λh model, and the non-random two liquid (NRTL) model were used to correlate the solubility of TCDNB. The calculated solubility data agreed well with the experimental data, and the modified Apelblat model fit best. Furthermore, the van't Hoff and Gibbs equations were also used to calculate the dissolution thermodynamic properties of TCDNB in various solvents. TCDNB dissolution could be an enthalpy-driven, non-spontaneous, and endothermic process in fifteen mono-solvents. The determination and fitting solubility of TCDNB, as well as the calculation of its thermodynamic properties, would be critical in the purification and crystallization of its preparation process research.

1. Introduction

Halopolynitroarenes are a type of chemical raw material or intermediate that is widely used in energy materials, medicine, dyes, pesticides, preservatives, and other fields [1]. Through the S_N-Ar reaction, a variety of substituents can be introduced into its structure [2]. The nitro and halogen atoms in its structure may be replaced depending on the activation degree of the substituent [3–8]. 2,3,4-trichloro-1,5-dinitrobenzene (TCDNB) is a halopolynitroarenes whose chemical molecular structure is shown in Fig. 1, which can be prepared by nitrification of 1,2,3-trichlorobenzene with a mixture of nitric and sulfuric acids [9]. 1,2,3-trichloro-4-nitrobenzene was obtained as a nitro by-product in the preparation of TCDNB [10]. The S_NAr reaction of TCDNB has been studied by some researchers [9,11,12], but the yield of the target product was low, and when the reaction reached its end point, the system might contain a small amount of unreacted raw materials. By-products will be produced whether the TCDNB is synthesized or other compounds are synthesized with TCDNB as a precursor, reducing the purity of the target product. As a result, in order to obtain a high-purity target product in the TCDNB production process, the reaction products must be separated and purified.

Among the many purification methods available, solution crystallization is a simple operation with a high purification efficiency. It is widely used and has a significant impact on substance purity and crystal quality [13,14]. The solid–liquid equilibrium data is generally expressed by solubility data, which is the basis of solution crystallization and can effectively improve the purity of the product [15,16]. However, there is no data on TCDNB solubility in the previously reported literature. As a result, in order to provide basic data to guide the purification and crystallization process of

* Corresponding author.
E-mail address: wangjianlong@nuc.edu.cn (J.-L. Wang).

https://doi.org/10.1016/j.cjche.2022.10.022
1004-9541/

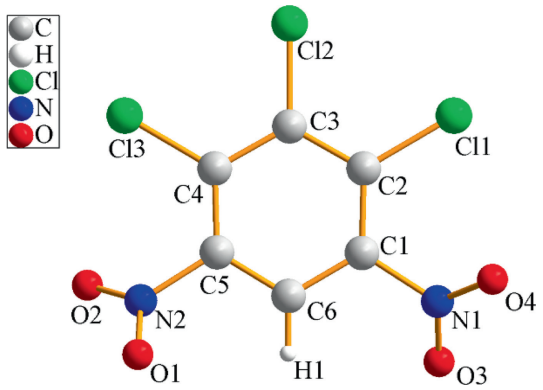

Fig. 1. Chemical molecular structure of TCDNB.

TCDNB, its solubility in various solvents must be measured [17]. The main impurities in the production of TCDNB are a small amount of unreacted raw materials and the mononitro by-product, 1,2,3-trichloro-4-nitrobenzene. The structural and physical properties of TCDNB influence the solvent selection.

Therefore, in this study, the solubility of TCDNB in methanol, ethanol, isopropanol, *n*-butanol, toluene, dichloromethane, chloroform, tetrachloromethane, 1,2-dichloroethane, acetone, ethyl acetate, acetonitrile, *N*-methylpyrrolidine (NMP), *N*,*N*-dimethylformamide (DMF), and dimethyl sulfoxide (DMSO) has been measured by a laser dynamic method at temperatures ranging from 278.15 to 323.15 K under 0.1 MPa. To investigate the effect of solvent effect on TCDNB solubility, the KAT-LSER model, which is based on the concept of linear solvation energy relationship, was used to fit TCDNB solubility data in different solvents at 298.15 K. Four solubility models were used to fit the experimental solubility of TCDNB in selected mono-solvents, including the van't Hoff model, modified Apelblat model, λh model, and non-random two-liquid (NRTL) model, extending the application of TCDNB solubility. Furthermore, using the Van Hoof equation and the Gibbs equation, the dissolution thermodynamic parameters such as the standard dissolution enthalpy, standard dissolution entropy, and standard Gibbs free energy of TCDNB in the corresponding solvents were calculated based on the experimental solubility data of TCDNB in selected mono-solvents.

2. Experimental

2.1. Materials

TCDNB was synthesized using a previous literature process [9], purified by repeated recrystallization in absolute ethanol, and its purity was greater than 0.995, as determined by high performance liquid chromatography (HPLC) (Fig. 2). All of the organic solvents used in the experiment are analytical grade reagents that were analyzed using gas chromatography. They were purchased from Sinopharm Chemical Reagent Co., Ltd., China. Table 1 provides detailed information on all of the materials used in this work.

2.2. Device and methods

The laser dynamics method was used to determine the solubility of TCDNB in selected mono-solvents, and its theory and device are described in Ref. [19,20]. The experimental devices, as shown in Fig. 3, are the same as those used to investigate the solubility of 1,3-dichloro-2,4,6-trinitrobenzene (DCTNB) in various mono-solvents [21].

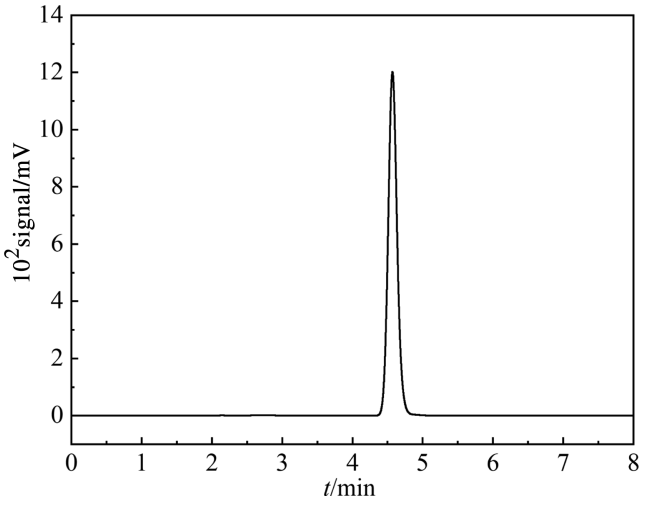

Fig. 2. HPLC analysis of TCDNB.

The experimental devices were set up as shown in Fig. 3 before the solubility test experiment. The following are the measurement steps: Turn on the laser transmitter, allow it to warm up for about 0.5 h, and then set the super constant temperature water bath to the desired temperature (standard uncertainty of temperature is 0.05 K). Add a certain amount of solvent to the jacketed crystallizer by pipette (standard uncertainty of 0.01 ml). Then, small amounts of TCDNB (solute) were added several times, stirring for 0.5 h after each addition. When the laser intensity received by the signal receiver is significantly reduced and there is visible undissolved solute in the jacketed crystallizer to the naked eye, the solute addition is stopped. Following that, a small amount of solvent was added several times with a pipette, stirring for 0.5 hours between additions. When the laser intensity remains stable for 0.5 h and does not change, it is considered that the solid–liquid equilibrium point has been reached and the solute has been completely dissolved in the system. The amount of solvent and solute added to the jacketed crystallizer at this time was recorded, and the mole fraction solubility of TCDNB (x_1) was calculated by Eq. (1). Each temperature point was measured three times in parallel, and the average value was taken as the final molar fraction solubility of TCDNB at this temperature point.

$$x_1 = \frac{m_1/M_1}{m_1/M_1 + m_2/M_2} \tag{1}$$

where m_1 and m_2 are the mass of TCDNB and solvent, respectively; M_1 and M_2 are the molar mass of TCDNB and solvent, respectively.

2.3. HPLC analysis

The purity of TCDNB was determined by HPLC (Shimadzu Corporation, LC-20AD, Japan). The chromatographic conditions for HPLC analysis are: column: Hypersil ODS2 column (250 mm × 4.6 mm, 5 μm), detection wavelength: 240 nm, mobile phase: $V_{methanol}$: V_{water} = 70: 30, flow rate: 1.2 ml·min^{-1}, column temperature: 298.15 K, injection volume: 10 μl.

2.4. Differential scanning calorimetry test

Thermal analysis was performed to determine the melting properties of TCDNB, including melting temperature (T_m) and enthalpy of fusion ($\Delta_{fus}H$), using a differential scanning calorimetry (DSC) apparatus (Mettler Toledo, model DSC 3, Switzerland) in this work. The reference material was indium, and the instrument was

Table 1
Detailed information of the materials used in this work

Chemical name	Molar mass/g·mol^{-1}	Mass faction purity	Analysis method	Solvent polarity③
TCDNB	271.44	>0.995	HPLC①	–
Methanol	32.04	>0.995	GC②	76.2
Ethanol	46.07	>0.995	GC②	65.4
Isopropanol	60.06	>0.995	GC②	54.6
n-Butanol	74.12	>0.995	GC②	60.2
Toluene	92.14	>0.995	GC②	9.90
Dichloromethane	84.93	>0.995	GC②	30.9
Chloroform	119.38	>0.995	GC②	25.9
Tetrachloromethane	153.84	>0.995	GC②	5.20
1,2-Dichloroethane	98.96	>0.995	GC②	32.7
Acetone	58.08	>0.995	GC②	35.5
Ethyl acetate	88.11	>0.995	GC②	23.0
Acetonitrile	41.06	>0.995	GC②	46.0
NMP	99.13	>0.995	GC②	36.0
DMF	73.09	>0.995	GC②	40.4
DMSO	78.13	>0.995	GC②	44.4

① High-performance liquid chromatography.
② Gas chromatography.
③ Solvent polarity was taken from Ref. [18].

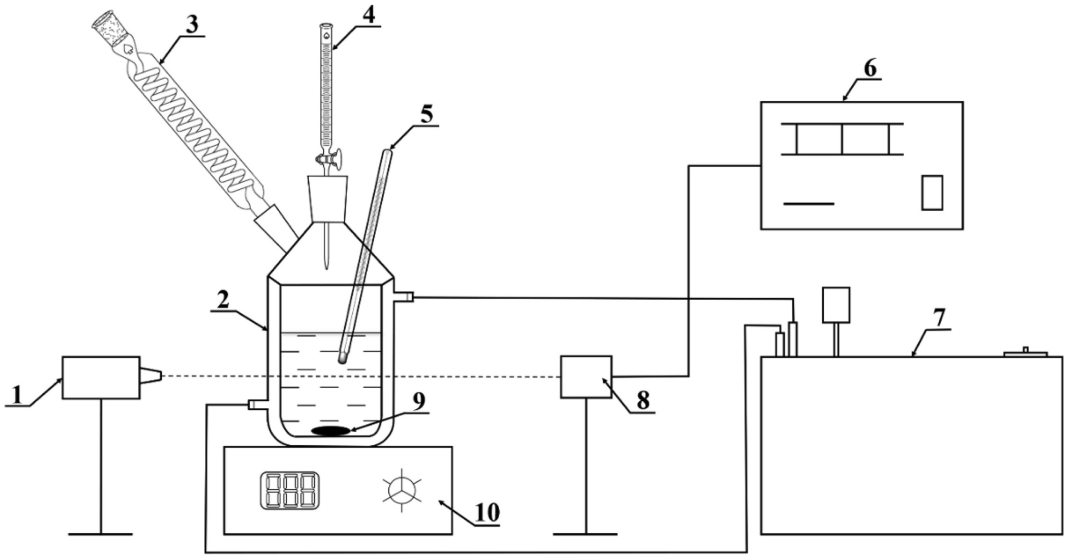

Fig. 3. Schematic diagram of the solubility measurement. 1—laser emitter; 2—crystallizer; 3—air condenser; 4—burette; 5—mercury thermometer; 6—display instrument; 7—super constant temperature water bath; 8—signal receiver; 9—magnetic rotor; 10—magnetic stirrer.

calibrated with standard indium and zinc before the determination. An open DSC pan containing 2 mg of TCDNB was heated from 323.15 to 393.15 K in the apparatus. Furthermore, the test conditions were as follows: N_2 atmosphere with a flow rate of 50 ml·min^{-1} and a heating rate of 10 K·min^{-1}. The test was repeated three times, with the average value being used.

2.5. Powder X-ray diffraction analysis

In order to determine whether TCDNB will change before and after the solubility measurement (chemical reaction, crystal transformation, production of solvate chemicals, *etc.*). A powder X-ray diffractometer (PXRD) (DX-2700B, Haoyuan Instrument Co., Ltd., China) was used to analyze the raw materials and the solid obtained from the solubility measurement. After the solubility test of TCDNB at the maximum temperature point, the system was cooled down and the solids were precipitated. After the system was cooled to room temperature, the solid obtained from the solubility measurement was obtained by vacuum filtration and drying at 40 °C. During the PXRD analysis, Cu K_α radiation (λ = 1.54 nm) was used, the tube voltage and current were 40 kV and 30 mA, respectively, the diffraction angle (2θ) ranged from 5° to 60°, the scanning rate was 5(°) ·min^{-1}, and the step size was 0.02°.

2.6. Solubility models

Many solubility models have been used in the study of solid–liquid phase equilibrium in recent years, due to the rapid development of theoretical foundations, and good application results have been obtained. To broaden the application of measured solubility data, the experimental solubilities of TCDNB in the selected mono-solvents were correlated in this study using four solubility models: the van't Hoff model, modified Apelblat model, λh model, and NRTL model.

2.6.1. van't Hoff model

The van't Hoff model is a well-known semi-empirical model that depicts the logarithm of the solute's mole fraction as linearly

related to the reciprocal of the absolute temperature in the ideal solution [22,23]. The van't Hoff model is expressed as Eq. (2):

$$\ln x_1 = A_1 + \frac{B_1}{T} \tag{2}$$

where x_1 is the mole fraction solubility of TCDNB; T is the absolute temperature; A_1 and B_1 are the model parameters related to the thermodynamic parameters of dissolved enthalpy and dissolved entropy.

2.6.2. Modified Apelblat model

The modified Apelblat model is a semi-empirical model that is widely used to represent the relationship between a compound's solubility in a mono-solvent or a mixed solvent and the absolute temperature [24,25]. The modified Apelblat model is expressed as Eq. (3):

$$\ln x_1 = A_2 + \frac{B_2}{T} + C_2 \ln T \tag{3}$$

where A_2, B_2, C_2 are the model parameters obtained by regressing experimental data.

2.6.3. λh model

The λh model, first proposed by Buchowski, is a semi-empirical model that can be used to correlate experimental solubility data for solid–liquid equilibrium systems [26,27]. The λh model is expressed as Eq. (4):

$$\ln\left[1 + \frac{\lambda(1-x_1)}{x_1}\right] = \lambda h\left(\frac{1}{T} + \frac{1}{T_m}\right) \tag{4}$$

where λ and h are the model parameters, stand for the association number of solute molecules in the non-ideal solution and the excess enthalpy of solution, respectively; T_m represents the melting temperature of TCDNB.

2.6.4. NRTL model

The NRTL model is a local composition requirements-based activity coefficient model that is commonly used to correlate and predict the solid–liquid equilibrium properties of most nonideal systems [28,29]. Renon proposed that the NRTL model, which can be simplified to Eq. (5), be used to calculate the thermodynamic properties of composition models.

$$\ln x_1 = \frac{\Delta_{fus}H}{R}\left(\frac{1}{T_m} - \frac{1}{T}\right) - \ln \gamma_1 \tag{5}$$

where $\Delta_{fus}H$ is the fusion enthalpy of TCDNB. In addition, γ_1 is the activity coefficient of a solute and can be calculated as Eq. (6):

$$\ln \gamma_1 = x_2^2\left[\frac{\tau_{21}G_{21}^2}{(x_1 + G_{21}x_2^2)} + \frac{\tau_{12}G_{12}^2}{(x_2 + G_{12}x_1^2)}\right] \tag{6}$$

where τ_{12}, τ_{21}, G_{12} and G_{21} can be calculated by Eqs. (7)–(10):

$$\tau_{12} = \frac{g_{12} - g_{22}}{RT} = \frac{\Delta g_{12}}{RT} \tag{7}$$

$$\tau_{21} = \frac{g_{21} - g_{11}}{RT} = \frac{\Delta g_{21}}{RT} \tag{8}$$

$$G_{12} = \exp(-\alpha\tau_{12}) \tag{9}$$

$$G_{21} = \exp(-\alpha\tau_{21}) \tag{10}$$

where Δg_{12} and Δg_{21} are the cross-interaction energies between the solute and the solvent molecules; α ranging from 0.20 to 0.47 is an adjustable parameter indicating the non-randomness of the solution and the recommended value of α is 0.3 in this system.

3. Results and Discussion

3.1. Melting properties of TCDNB

Fig. 4 shows the DSC curve of TCDNB. Through the integral analysis of the DCS curve obtained by three thermal analyses, the T_m and $\Delta_{fus}H$ of TCDNB were obtained to be (365.91 ± 0.31) K and (25.57 ± 0.27) kJ·mol^{-1}, respectively. The T_m data in this study is consistent with the values reported in the previous literature [9]. The uncertainty type of the T_m and $\Delta_{fus}H$ was standard uncertainty u (0.68 confidence level), and the uncertainty values were 0.31 K and 0.27 kJ·mol^{-1}, respectively.

3.2. Powder X-ray diffraction analysis

The PXRD patterns of the equilibrium solid phases obtained from the solubility measurement and the raw materials are shown in Fig. 5. It can be seen from Fig. 5 that in all selected mono-solvent systems, the PXRD patterns of the equilibrium solid phase obtained from the solubility measurement are consistent with those of the raw material, and there is no peak shift. The results of PXRD analysis indicated that there was no solvate formation and polymorph conversion during the solubility measurement process [30].

3.3. Solubility data of TCDNB

The experimental mole fraction solubility data (x_1^{exp}) and calculated solubility values (x_1^{cal}) by the modified Apelblat model of TCDNB are listed in Table 2 and presented graphically in Fig. 6, which are in fifteen mono-solvents of methanol, ethanol, isopropanol, *n*-butanol, toluene, dichloromethane, chloroform, tetrachloromethane, 1,2-dichloroethane, acetone, ethyl acetate, acetonitrile, NMP, DMF, DMSO at a temperature of 278.15–323.15 K under 0.1 MPa. It can be seen that the solubility of TCDNB in all selected mono-solvents increases when the temperature increases, indicating that the dissolution of TCDNB is an endothermic process. In addition, it can be seen from Fig. 6(a) that the solubility curves of TCDNB in methanol and *n*-butanol have an intersection point around 308.15 K. When the temperature is lower than 308.15 K, the solubility of TCDNB in methanol is greater than in *n*-butanol, while the opposite is true when the temperature is higher than 308.15 K. This indicates that the effect of temperature on the solubility of TCDNB is different in different mono-solvent systems.

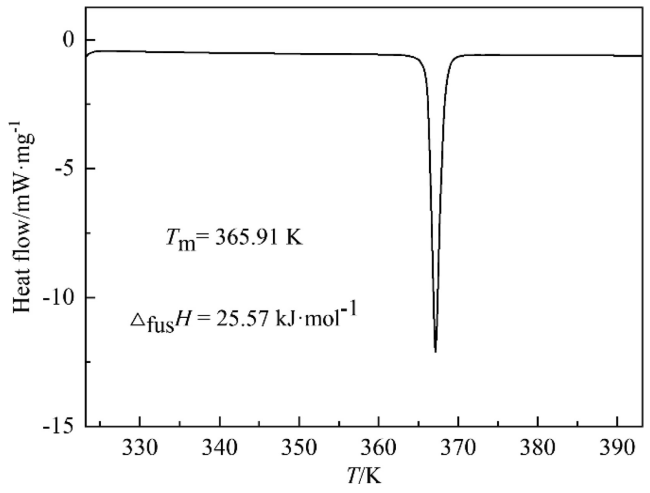

Fig. 4. DSC curve of TCDNB.

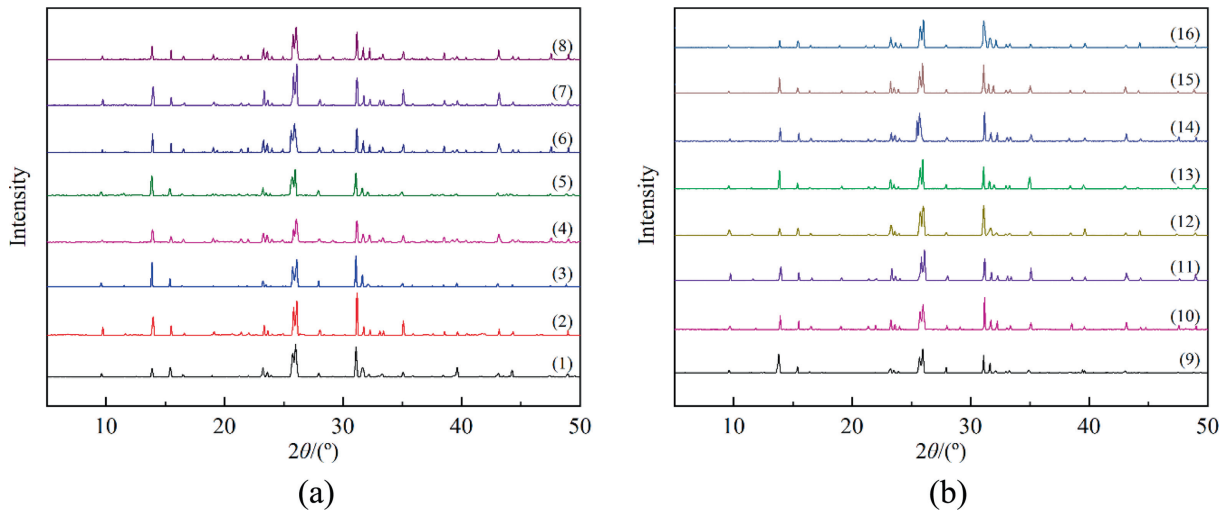

Fig. 5. The P-XRD patterns of raw material and equilibrium solid phases of TCDNB in fifteen mono-solvents. (a): (1) raw material; (2) methanol; (3) ethanol; (4) isopropanol; (5) *n*-butanol; (6) toluene; (7) dichloromethane; (8) chloroform; (b): (9) tetrachloromethane; (10) 1,2-dichloroethane; (11) acetone; (12) ethyl acetate; (13) acetonitrile; (14) NMP; (15) DMF; (16) DMSO.

Table 2
Experimental mole fraction solubility (x_1^{exp}) and calculated solubility values (x_1^{cal}) by the modified Apelblat model of TCDNB in fifteen mono-solvents at the temperature from 278.15 to 313.15 K under 0.1 MPa

T/K	Methanol		Ethanol		Isopropanol		*n*-Butanol		Toluene	
	$10^2x_1^{exp}$	$10^2x_1^{cal}$	$10^2x_1^{exp}$	$10^2x_1^{cal}$	$10^2x_1^{exp}$	$10^2x_1^{cal}$	$10^2x_1^{exp}$	$10^2x_1^{cal}$	$10^2x_1^{exp}$	$10^2x_1^{cal}$
278.15	0.2623	0.2634	0.2351	0.2368	0.0879	0.0897	0.1751	0.1767	13.99	13.99
283.15	0.3298	0.3315	0.3012	0.3017	0.1248	0.1259	0.2385	0.2388	15.91	15.91
288.15	0.4137	0.4155	0.3818	0.3827	0.1743	0.1751	0.3201	0.3205	18.04	18.04
293.15	0.5188	0.5186	0.4827	0.4835	0.2406	0.2415	0.4275	0.4272	20.39	20.38
298.15	0.6482	0.6449	0.6107	0.6084	0.3333	0.3303	0.5652	0.5656	22.99	22.97
303.15	0.8063	0.7990	0.7650	0.7626	0.4513	0.4482	0.7524	0.7441	25.77	25.80
308.15	0.9847	0.9864	0.9565	0.9524	0.6031	0.6037	0.9674	0.9730	28.92	28.91
313.15	1.207	1.214	1.183	1.185	0.807	0.807	1.262	1.265	32.29	32.31
318.15	1.488	1.488	1.461	1.470	1.069	1.072	1.637	1.635	36.02	36.01
323.15	1.821	1.819	1.821	1.816	1.417	1.415	2.102	2.102	40.05	40.05

T/K	Dichloromethane		Chloroform		Tetrachloromethane		1,2-Dichloroethane		Acetone	
	$10^2x_1^{exp}$	$10^2x_1^{cal}$	$10^2x_1^{exp}$	$10^2x_1^{cal}$	$10^2x_1^{exp}$	$10^2x_1^{cal}$	$10^2x_1^{exp}$	$10^2x_1^{cal}$	$10^2x_1^{exp}$	$10^2x_1^{cal}$
278.15	6.887	6.888	5.363	5.370	0.3743	0.3707	6.005	5.986	10.90	10.90
283.15	8.221	8.221	6.601	6.604	0.5819	0.5796	7.355	7.346	12.42	12.42
288.15	9.752	9.761	8.069	8.068	0.8908	0.8910	8.950	8.952	14.12	14.11
293.15	11.56	11.53	9.816	9.795	1.344	1.348	10.82	10.83	15.98	15.99
298.15	13.54	13.56	11.85	11.82	2.012	2.008	13.02	13.03	18.10	18.08
303.15	15.89	15.88	14.13	14.18	2.959	2.948	15.54	15.58	20.36	20.39
308.15	18.52	18.51	16.91	16.93	4.251	4.270	18.50	18.51	22.94	22.94
313.15	–	–	20.14	20.10	6.093	6.103	21.94	21.88	25.74	25.76
318.15	–	–	23.74	23.75	8.637	8.615	25.75	25.73	28.89	28.86
323.15	–	–	27.92	27.92	12.01	12.02	30.08	30.10	32.27	32.28

T/K	Ethyl acetate		Acetonitrile		NMP		DMF		DMSO	
	$10^2x_1^{exp}$	$10^2x_1^{cal}$	$10^2x_1^{exp}$	$10^2x_1^{cal}$	$10^2x_1^{exp}$	$10^2x_1^{cal}$	$10^2x_1^{exp}$	$10^2x_1^{cal}$	$10^2x_1^{exp}$	$10^2x_1^{cal}$
278.15	9.696	9.682	4.012	4.020	27.80	27.87	19.44	19.44	–	–
283.15	11.14	11.14	5.108	5.113	29.15	29.11	21.15	21.16	–	–
288.15	12.77	12.78	6.445	6.447	30.53	30.51	23.03	23.04	–	–
293.15	14.61	14.62	8.063	8.061	32.13	32.07	25.08	25.09	23.81	23.80
298.15	16.69	16.70	10.02	10.00	33.80	33.79	27.41	27.33	26.17	26.17
303.15	19.05	19.03	12.32	12.31	35.72	35.69	29.79	29.76	28.73	28.74
308.15	21.67	21.64	15.05	15.05	37.71	37.78	32.39	32.41	31.49	31.52
313.15	24.51	24.56	18.26	18.28	40.05	40.08	35.22	35.29	34.54	34.52
318.15	27.85	27.81	22.03	22.05	42.55	42.60	38.37	38.43	37.80	37.76
323.15	31.41	31.43	26.45	26.44	45.42	45.36	41.90	41.84	41.22	41.24

Note: Due to the fact that the boiling point of dichloromethane is 312.90 K and the freezing point of DMSO is 291.55 K, the temperature point and quantity are adjusted accordingly when measuring the solubility of TCDNB in these two solvents.
The relative standard uncertainty of the solubility is $u_r(x_1) = 0.05$; the standard uncertainties are $u(T) = 0.1$ K, $u(p) = 0.02$ MPa.

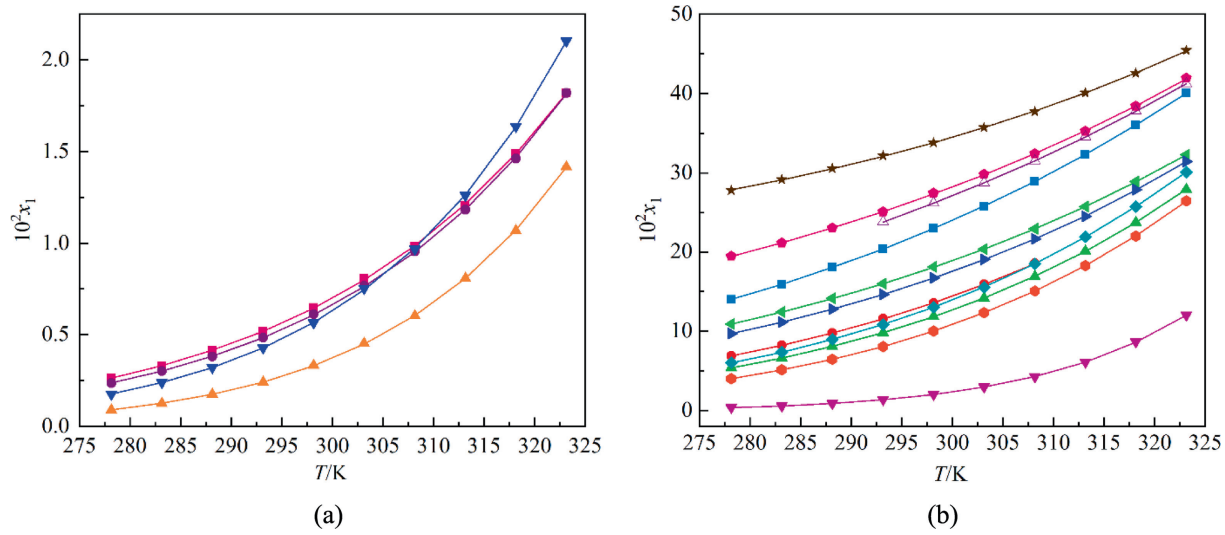

Fig. 6. The mole fraction solubility (x_1) of TCDNB in fifteen mono-solvents at the temperature from 278.15 to 323.15 K under 0.1 MPa: (a) ■, methanol; ●, ethanol; ▲, isopropanol; ▼, *n*-butanol; (b) ■, toluene; ●, dichloromethane; ▲, chloroform; ▼, tetrachloromethane; ◆, 1,2-dichloroethane; ◄, acetone; ▲, ethyl acetate; ◇, acetonitrile; ★, NMP; ◇, DMF; △, DMSO; solid lines are calculated curves by the modified Apelblat model.

When the temperature is 298.15 K, the order of the experimental mole fraction solubility (x_1^{exp}) of TCDNB in the selected mono-solvent is isopropanol (0.003333) < *n*-butanol (0.005652) < ethanol (0.006107) < methanol (0.006482) < tetrachloromethane (0.0201 2) < acetonitrile (0.1002) < chloroform (0.1185) < 1,2-dichloroe thane (0.1302) < dichloromethane (0.1354) < ethyl acetate (0.166 9) < acetone (0.1810) < toluene (0.2299) < DMSO (0.2617) < DMF (0.2741) < NMP (0.3380). However, the order of polarity of the selected mono-solvents is aprotic solvent (tetrachloromethane (5.20), toluene (9.90), ethyl acetate (23.0), chloroform (25.9), dichloromethane (30.9), and 1,2-dichloroethane (32.7)) < dipolar parent solvents (acetone (35.5), NMP (36.0), DMF (40.4), DMSO (44.4), and acetonitrile (46.0)) < alcohols (isopropanol (54.6), *n*-butanol (60.2), ethanol (65.4), and methanol (76.2)). This indicates that the order of TCDNB solubility in all selected mono-solvents is inconsistent with the order of solvent polarity. This phenomenon shows that the dissolution process of TCDNB in the selected mono-solvent is not only affected by the polarity of the solvent but may be affected by multiple factors, such as molecular structure, functional groups, van der Waals forces, solvation and other properties of the solvent, *etc.*

3.4. Solvent effects: KAT-LSER model

Kallet *et al.* [31,32] proposed the KAT-LSER model based on the linear solvation energy relationships (LSER) concept. This model can relate the solubility of a substance to the properties of a mono-solvent, so as to understand the influence of the types, directions, and extent of various interactions on solvent effects in solid–liquid equilibrium. Eq. (11) is the calculation formula of the KAT-LSER model.

$$\ln x_1 = c_0 + c_1\alpha + c_2\beta + c_3\pi^* + c_4\left(\frac{V_s\delta_H^2}{100RT}\right) \tag{11}$$

where α is the hydrogen bond acidity of solvents, β is the hydrogen bonding basicity of solvents, π^* is the dipolarity/polarizability of solvents, and δ_H is the Hildebrand solubility parameter of solvents; v_s is the molar volume of the solute and its calculation formula is as Eq. (12), and its calculated value is 136.90 $cm^3 \cdot mol^{-1}$; R is the gas constant (8.3145 $J \cdot mol^{-1} \cdot K^{-1}$). Moreover, c_0 refers to the intercept at $\alpha = \beta = \pi^* = \delta_H = 0$; c_1 and c_2 denote the solute's susceptibility to the specific solute–solvent interactions; c_3 and c_4 denote the sensitivity of the solubility to the nonspecific solute–solvent and solvent–solvent interactions, respectively [33].

$$v_s = M/\rho \tag{12}$$

where v_s is the molar volume of the solute, M is the relative molecular mass of the solute, and ρ is the density of the solute.

The parameter values of α, β, π^* and δ_H for all selected mono-solvents in the experiment are shown in Table 3. The KAT-LSER model was fitted by using Origin 2018 software via multiple linear regression analysis (MLRA) and the result is shown in Eq. (13).

$$\ln x_1 = -2.37 - 2.17\alpha + 0.85\beta + 0.63\pi^* - 1.40\left(\frac{v_s\delta_H^2}{100RT}\right) \tag{13}$$

$$\text{RMSD} = 0.0224, \quad R^2 = 0.9469, \quad F = 231.6096$$

The value of R^2 approached 1, and the low values of RMSD indicated that the model had a good fitting effect. F is the F-test.

It can be seen from the negative coefficient of α that the hydrogen bond acidity of the selected mono-solvent is not conducive to the dissolution of TCDNB, while the coefficients of β and π^* are positive, indicating that the hydrogen bond basicity and dipolarity/polarizability of the solvent are conducive to the dissolution of TCDNB. Moreover, the negative value of c_4 indicates that the solvent–solvent interaction makes the solution have higher self-cohesiveness, which was not conducive to the dissolution of TCDNB. In addition, according to the proportion of all coefficients and absolute values of constant terms in Eq. (13), the proportions of α, β, π^* and δ_H in the total solvent effect are 0.293, 0.115, 0.085, and 0.188, respectively, so the order of their influence on the solubility of TCDNB is: $\alpha > \delta_H > \beta > \pi^*$. It showed that for the solubility of TCDNB in all selected mono-solvents, the hydrogen bond acidity of the solvent has a significant influence, the solvent–solvent interactions have a great influence, the hydrogen bonding basicity has a relatively small influence, and the polarity / polarizability has the smallest influence. In addition, for alcohol solvents, the value of α is methanol > ethanol > *n*-butanol > isopro panol, while the corresponding TCDNB solubility order is the same, which shows that the significant effect of hydrogen bond acidity on the solubility of TCDNB is not obvious when the value of α is large, which again shows that the solubility of TCDNB in the solvent is the result of the combined action of many factors.

Table 3
Values of α, β, π^* and δ_H for the fifteen mono-solvents

Solvents	α[①]	β[①]	π^*[①]	δ_H[②]/MPa$^{1/2}$
Methanol	0.98	0.66	0.60	22.30
Ethanol	0.86	0.75	0.54	19.40
Isopropanol	0.76	0.84	0.48	16.40
n-Butanol	0.84	0.84	0.47	15.80
Toluene	0.00	0.11	0.55	2.00
Dichloromethane	0.13	0.10	0.82	6.10
Chloroform	0.20	0.10	0.58	5.70
Tetrachloromethane	0.00	0.10	0.28	0.60
1,2-Dichloroethane	0.00	0.10	0.81	4.10
Acetone	0.08	0.48	0.71	7.00
Ethyl acetate	0.00	0.45	0.55	7.20
Acetonitrile	0.19	0.40	0.75	24.40
NMP	0.00	0.77	0.92	7.20
DMF	0.00	0.69	0.88	11.30
DMSO	0.00	0.752	1.00	10.20

① α, β, and π^* was taken from Ref. [34].
② δ_H was taken from Ref. [35], and T = 298.15 K.

Table 4
The values of model parameters, ARD and RMSD obtained using four solubility models

Model	Parameter	Methanol	Ethanol	Isopropanol	*n*-Butanol	Toluene
van't Hoff	A_2	8.21	8.90	13.07	11.74	5.63
	B_2	−3951.24	−4173.00	−5601.76	−5043.21	−2115.65
	10^2ARD	1.24	1.41	1.06	1.32	0.37
	10^3RMSD	0.09	0.09	0.04	0.07	0.95
Modified Apelblat	A_1	−76.63	−81.92	−47.66	−58.56	−20.81
	B_1	−81.52	−26.23	−2809.16	−1819.22	−921.04
	C_1	12.61	13.50	9.02	10.44	3.94
	10^2ARD	0.37	0.34	0.60	0.34	0.04
	10^3RMSD	0.04	0.04	0.02	0.03	0.13
λh	λ	4.17×10^{-2}	4.79×10^{-2}	8.04×10^{-2}	9.16×10^{-2}	0.64
	h	77111.39	72836.15	64298.61	49634.82	2868.13
	10^2ARD	1.68	1.46	1.70	1.44	0.18
	10^3RMSD	0.11	0.09	0.04	0.08	0.53
NRTL	Δg_{12}	13606.82	7683.80	−1867.29	63498.37	−3119.37
	Δg_{21}	3447.87	3316.82	5848.98	4661.14	1666.58
	α	0.30	0.30	0.30	0.30	0.30
	10^2ARD	0.97	0.55	0.78	0.66	0.17
	10^3RMSD	0.06	0.04	0.02	0.04	0.45

Model	Parameter	Dichloromethan	Chloroform	Tetrachloromethane	1,2-Dichloroethane	Acetone
van't Hoff	A_2	7.51	8.95	19.20	8.78	5.65
	B_2	−2833.07	−3304.49	−6888.59	−3226.53	−2192.65
	10^2ARD	0.18	0.25	0.76	0.14	0.60
	10^3RMSD	0.24	0.35	0.15	0.25	1.18
Modified Apelblat	A_1	−14.16	−3.39	52.28	8.32	−36.11
	B_1	−1876.87	−2743.35	−8418.18	−3205.31	−305.51
	C_1	3.24	1.84	−4.91	6.95E-02	6.22
	10^2ARD	0.09	0.15	0.31	0.13	0.06
	10^3RMSD	0.16	0.27	0.11	0.25	0.15
λh	λ	0.67	0.87	1.65	0.95	0.41
	h	3972.35	3714.61	4274.05	3360.94	4135.07
	10^2ARD	0.14	0.18	0.72	0.10	0.49
	10^3RMSD	0.19	0.29	0.14	0.28	1.10
NRTL	Δg_{12}	9570.03	56591.99	−13434.57	1065.67	27886.66
	Δg_{21}	−6213.63	583.79	13551.55	−603.13	−2791.70
	α	0.30	0.30	0.30	0.30	0.30
	10^2ARD	0.25	0.26	1.16	0.27	1.62
	10^3RMSD	0.33	0.33	0.19	0.48	3.14

Model	Parameter	Ethyl acetate	Acetonitrile	NMP	DMF	DMSO
van't Hoff	A_2	6.22	10.28	2.29	3.94	4.51
	B_2	−2386.56	−3752.07	−1000.25	−1559.83	−1744.59
	10^2ARD	0.78	0.20	1.31	0.90	0.26
	10^3RMSD	1.39	0.18	5.29	2.96	0.91
Modified Apelblat	A_1	−46.52	19.88	−98.15	−65.20	−36.96
	B_1	−0.29	−4189.32	3510.84	1554.92	158.47

(*continued on next page*)

Table 4 (*continued*)

Model	Parameter	Methanol	Ethanol	Isopropanol	*n*-Butanol	Toluene
	C_1	7.85	−1.43	14.97	10.30	6.16
	10^2ARD	0.11	0.08	0.12	0.12	0.06
10^3RMSD	0.26	0.10	0.48	0.46	0.24	
λh	λ	0.48	1.07	−0.11	0.26	0.33
	h	4077.99	3541.07	3538.25	3241.70	3182.10
	10^2ARD	0.24	0.10	0.06	0.19	0.25
	10^3RMSD	0.58	0.11	0.24	0.61	0.94
NRTL	Δg_{12}	32600.92	−1393.10	−12257.95	−6067.30	−18460.83
	Δg_{21}	−1605.95	2252.61	6218.52	3914.59	24013.62
	α	0.30	0.30	0.30	0.30	0.30
	10^2ARD	1.61	1.08	0.20	0.43	0.29
	10^3RMSD	2.85	1.01	0.79	1.49	1.30

3.5. Evaluation of solubility models

The average relative deviation (ARD) and root mean square deviation (RMSD) were used to evaluate the accuracy of the selected models mentioned above. The formulas for ARD and RMSD are shown in Eqs. (14) and (15).

$$\mathrm{ARD} = \frac{1}{N}\sum_{i=1}^{N}\left|\frac{x_i^{\mathrm{exp}} - x_i^{\mathrm{cal}}}{x_i^{\mathrm{exp}}}\right| \tag{14}$$

$$\mathrm{RMSD} = \left[\frac{1}{N}\sum_{i=1}^{N}\left(x_i^{\mathrm{exp}} - x_i^{\mathrm{cal}}\right)^2\right]^{1/2} \tag{15}$$

where N is the total number of experiment points in each mono-solvent.

The parameters of the four selected models, along with ARD and RMSD, are listed in Table 4. It can be seen from Table 4 that for the selected model, all 10^2ARD values are less than 1.70, and the average values are 0.72 (van't Hoff), 0.19 (modified Apelblet), 0.60 (λh), 0.69 (NRTL); all 10^3RMSD values were less than 5.30, and the average values were 0.94 (van't Hoff), 0.18 (modified Apelblet), 0.35 (λh), and 0.83 (NRTL). The calculated results show that the ARD and RMSD of the four solubility models are all small, indicating good agreement with the experimental data. Among the four models, the modified Apelblat model has the best correlation.

3.6. Thermodynamic parameters of dissolution

In the solid–liquid equilibrium system, the study of thermodynamic properties is helpful to understand the dissolution behavior of TCDNB in selected mono-solvents. The thermodynamic parameters of dissolution mainly include standard dissolution enthalpy ($\Delta H_{\mathrm{dis}}^0$), standard dissolution entropy ($\Delta S_{\mathrm{dis}}^0$), and standard Gibbs free energy ($\Delta G_{\mathrm{dis}}^0$). The analysis of dissolution thermodynamic parameters is conductive to understanding the variety of TCDNB solubility, which can be calculated by the van't Hoff and Gibbs equations, whose calculation equations are shown in Eqs. (16) and (17) [36–38].

$$\ln x_1 = -\frac{\Delta H_{\mathrm{dis}}^0}{RT} + \frac{\Delta S_{\mathrm{dis}}^0}{R} \tag{16}$$

$$\Delta G_{\mathrm{dis}}^0 = \Delta H_{\mathrm{dis}}^0 - T_{\mathrm{mean}}\Delta S_{\mathrm{dis}}^0 \tag{17}$$

Here $\Delta H_{\mathrm{dis}}^0$ and $\Delta S_{\mathrm{dis}}^0$ can be calculated from the slope and intercept of the lines fitted by the van't Hoff equation, respectively [39], as shown in Eqs. (18) and (19); T_{mean} is the mean harmonic temperature, and the value is 299.96 K in this work, which was calculated as Eq. (20):

$$\Delta H_{\mathrm{dis}}^0 = -R \times \mathrm{slope} \tag{18}$$

$$\Delta S_{\mathrm{dis}}^0 = R \times \mathrm{intercept} \tag{19}$$

$$T_{\mathrm{mean}} = \frac{N}{\sum_{i=1}^{N}\frac{1}{T_i}} \tag{20}$$

where N represents the number of measurement temperature points for any selected mono-solvent, T_i represents the measurement temperature from 278.15 to 323.15 K.

It can be seen from Eq. (17) that the $\Delta G_{\mathrm{dis}}^0$ will be affected by the relative sizes of $\Delta H_{\mathrm{dis}}^0$ and $\Delta S_{\mathrm{dis}}^0$ during the dissolution process. Therefore, the driving force of the dissolution process is divided into two types: enthalpy-driven and entropy-driven, which are represented by enthalpy contribution (ξ_H) and entropy contribution (ξ_S), respectively [40,41], and the calculation equations of the two are as Eqs. (21) and (22):

$$\xi_H = \frac{\left|\Delta H_{\mathrm{dis}}^0\right|}{\left|\Delta H_{\mathrm{dis}}^0\right| + \left|T_{\mathrm{mean}}\Delta S_{\mathrm{dis}}^0\right|} \times 100\% \tag{21}$$

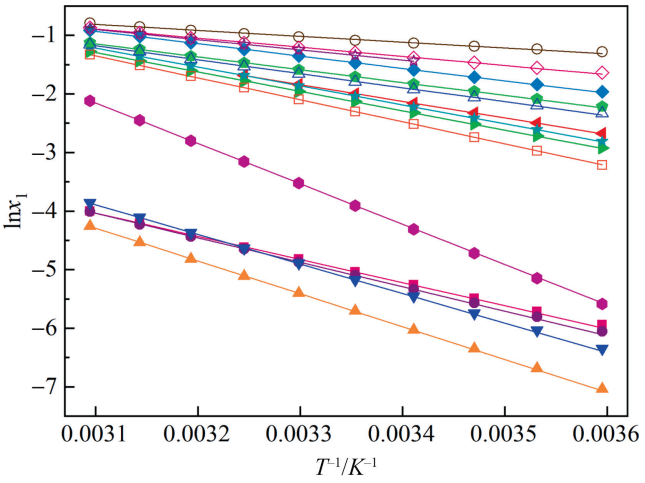

Fig. 7. The relationship between ln$x$ and $1/T$ of TCDNB in fifteen mono-solvents at temperature from 278.15 K to 323.15 K under 0.1 MPa: ■, methanol; ●, ethanol; ▲, isopropanol; ▼, *n*-butanol; ◆, toluene; ◄, dichloromethane; ▲, chloroform; ◇, tetrachloromethane; ★, 1,2-dichloroethane; ◇, acetone; △, ethyl acetate; □, acetonitrile; ○, NMP; ◇, DMF; ☆, DMSO; solid lines are calculated curves by van't Hoff model.

Table 5
The thermodynamic properties of TCDNB in fifteen mono-solvents at mean temperature (299.96 K) under 0.1 MPa

Solvent	ΔH^0_{dis}/kJ · mol^{-1}	ΔS^0_{dis}/J · K^{-1} · mol^{-1}	ΔG^0_{dis}/kJ · mol^{-1}	ξ_H/%	ξ_S/%
Methanol	32.85	68.29	12.37	61.59	38.41
Ethanol	34.70	73.98	12.50	60.99	39.01
Isopropanol	46.58	108.70	13.97	58.82	41.18
n-Butanol	41.93	97.61	12.65	58.88	41.12
Toluene	17.59	46.80	3.55	55.62	44.38
Dichloromethane	23.56	62.41	5.28	56.31	43.69
Chloroform	27.48	74.41	5.16	55.18	44.82
Tetrachloromethane	57.28	159.63	9.39	54.47	45.53
1,2-Dichloroethane	26.83	73.03	4.92	55.05	44.95
Acetone	18.23	46.97	4.14	56.41	43.59
Ethyl acetate	19.84	51.73	4.33	56.12	43.88
Acetonitrile	31.20	85.48	5.55	54.89	45.11
NMP	8.32	19.00	2.62	59.33	40.67
DMF	12.97	32.80	3.13	56.87	43.13
DMSO	14.51	37.50	2.96	55.69	44.31

$$\xi_S = \frac{\left|T_{mean}\Delta S^0_{dis}\right|}{\left|\Delta H^0_{dis}\right| + \left|T_{mean}\Delta S^0_{dis}\right|} \times 100\% \quad (22)$$

The relationship curve between logarithm of mole fraction solubility ($\ln x_1$) and ($1/T$) for TCDNB in all selected mono-solvents at different temperatures is shown in Fig. 7. The values of thermodynamic parameters (ΔH^0_{dis}, ΔS^0_{dis}, ΔG^0_{dis}, ξ_H, and ξ_S) for TCDNB dissolved in all selected mono-solvents are listed in Table 5. As shown in Table 5, all the values of ΔH^0_{dis} and ΔG^0_{dis} are both positive, indicating that the dissolution behavior of TCDNB in all selected mono-solvents is a non-spontaneous and endothermic process [42]. Moreover, the values of ΔS^0_{dis} are all positive, indicating that the dissolution of TCDNB in all selected mono-solvents is an entropy-increasing process.

Moreover, when the value of ΔG^0_{dis} is smaller, the solid–liquid equilibrium system is more stable, the non-volume work required for dissolution is smaller, and the solubility of the substance is larger in the system. As can be seen from Table 5, the order of ΔG^0_{dis} values are: isopropanol > *n*-butanol > ethanol > methanol > tetrachloromethane > acetonitrile > dichloromethane > chloroform > 1,2-dichloroethane > ethyl acetate > acetone > toluene > DMF > DMSO > NMP. This also shows again that TCDNB has the smallest molar solubility in isopropanol and the largest molar solubility in NMP. Furthermore, the values of all ξ_H are greater than ξ_S and more than 54.46%, which indicates that the driving force for the dissolution process of TCDNB in all selected mono-solvents is enthalpy-driven.

4. Conclusions

In this work, the laser dynamic method was employed to measure the solubility of TCDNB in fifteen mono-solvents. The measurement results showed that the solubility of TCDNB increased with the increase of temperature. The molar fraction solubility (x_1) of TCDNB decreases in the order of NMP, DMF, DMSO, toluene, acetone, ethyl acetate, dichloromethane, 1,2-dichloroethane, chloroform, acetonitrile, tetrachloromethane, methanol, ethanol, *n*-butanol, and isopropanol at 298.15 K. The effect of solvent parameters on the solubility of TCDNB was investigated by correlating the solubility data using the KAT-LSER model. The results show that the hydrogen bond acidity of the solvent and the solvent–solvent interaction are both unfavorable to the dissolution of TCDNB and have a greater degree of influence; while the hydrogen bond basicity and dipolarity/polarizability of the solvent are favorable to the dissolution of TCDNB, the influence is relatively small. The experimental solubility of TCDNB was successfully correlated by the van't Hoff model, the modified Apelblat model, the λh model, and the NRTL model, with the Apelblat equation providing the best fitting results. In addition, the dissolution thermodynamic parameters of TCDNB in all selected mono-solvents were calculated, and the results showed that the dissolution of TCDNB is a non-spontaneous and endothermic process. The solubility data, correlation models, and thermodynamic parameters can provide a basis for the study of the crystallization and purification process of TCDNB.

Declaration of Competing Interest

The authors declare that they have no known competing financial interests or personal relationships that could have appeared to influence the work reported in this paper.

Supplementary Material

Supplementary data to this article can be found online at https://doi.org/10.1016/j.cjche.2022.10.022.

References

[1] M. Pietrowski, Recent developments in heterogeneous selective hydrogenation of halogenated nitroaromatic compounds to halogenated anilines, *Curr. Org. Synth.* 9 (4) (2012) 470–487.
[2] R.S. Begunov, P.D. Gopanyuk, A.A. Sokolov, V.O. Sakulina, SNAr reaction of 1, 5-dichloro-2, 4-dinitrobenzene with S-, O-, and N-nucleophiles, *Russ. J. Org. Chem.* 54 (6) (2018) 945–948.
[3] M.D. Senskey, J.D. Bradshaw, C.A. Tessier, W.J. Youngs, Aryl nitro group substitution by primary and secondary amines, *Tetrahedron Lett.* 36 (35) (1995) 6217–6220.
[4] N.V. Zotova, P.M. Kushakova, V.A. Kuznetsov, A.A. Rodin, A.V. Garabadzhiu, Specific features of nucleophilic substitution in 1-chloro-3, 4-dinitrobenzene, *Russ. J. Org. Chem.* 40 (10) (2004) 1473–1476.
[5] N.V. Zotova, P.M. Kushakova, V.A. Kuznetsov, A.A. Rodin, A.V. Garabadzhiu, Regular trends in nucleophilic substitutions in 2-alkylamino-4-chloronitrobenzenes, *Russ. J. Org. Chem.* 41 (2) (2005) 214–217.
[6] F.G. Menezes, J. Ricardo, R. Dias, A.J. Bortoluzzi, C. Zucco, Reações de 1, 2-dicloro-4, 5-dinitrobenzeno com aminas: monossubstituição de nitro e dissubstituição de cloro e nitro, *Quím. Nova* 30 (2) (2007) 356–359.
[7] N.A. Senger, B. Bo, Q. Cheng, J.R. Keeffe, S. Gronert, W.M. Wu, The element effect revisited: factors determining leaving group ability in activated nucleophilic aromatic substitution reactions, *J. Org. Chem.* 77 (21) (2012) 9535–9540.
[8] A. Blaskó, C.A. Bunton, N.D. Gillitt, R. Bacaloglu, S.F. Yunes, C. Zucco, The reaction of 1, 2-dichloro-4, 5-dinitrobenzene with hydroxide ion: roles of meisenheimer complexes and radical pairs, *J. Braz. Chem. Soc.* 24 (2013) 1146–1159.
[9] E.H. Huntress, F.H. Carten, Identification of organic compounds. I. chlorosulfonic acid as a reagent for the identification of aryl halides, *J. Am. Chem. Soc.* 62 (3) (1940) 511–514.
[10] R.B. Moodie, R.J. Stephens, Electrophilic aromatic substitution. Part 33. Kinetics and products of aromatic nitrations in solutions of dinitrogen pentaoxide in nitric acid, *J. Chem. Soc., Perkin Trans.* 2 (8) (1987) 1059.

[11] Y. Gimbert, A. Moradpour, C. Merienne, Regiochemical effects associated with nucleophilic aromatic substitutions by bidentate sulfur nucleophiles, *J. Org. Chem.* 55 (19) (1990) 5347–5350.
[12] B. Mahiou, M.L. Deinzer, Synthetic strategies in the preparation of regiospecifically chlorine-37 labeled polychlorinated dibenzo-p-dioxins, *J. Label. Compd. Radiopharm.* 31 (4) (1992) 261–287.
[13] Z.R. Wang, G.Y. Zhou, J.J. Dong, Z.L. Li, L. Ding, B.H. Wang, Measurement and correlation of the solubility of antipyrine in ten pure and water + ethanol mixed solvents at temperature from (288.15 to 328.15) K, *J. Mol. Liq.* 268 (2018) 256–265.
[14] B.J. Fan, Q.S. Li, Y.F. Li, X.L. Song, J.P. Yin, Solubility measurement and correlation for 1-naphthoic acid in nine pure and binary mixed solvents from *T* = (293.15 to 333.15) K, *J. Mol. Liq.* 273 (2019) 58–67.
[15] L. Ding, B.H. Wang, F. Wang, J.J. Dong, G.Y. Zhou, H.X. Li, Measurement and correlation of the solubility of dipyrone in ten mono and water + ethanol mixed solvents at temperatures from (293.15 to 332.85) K, *J. Mol. Liq.* 241 (2017) 742–750.
[16] F. Saadatfar, A. Shayanfar, E. Rahimpour, M. Barzegar-Jalali, F. Martinez, M. Bolourtchian, A. Jouyban, Measurement and correlation of clotrimazole solubility in ethanol + water mixtures at *T* = (293.2 to 313.2) K, *J. Mol. Liq.* 256 (2018) 527–532.
[17] L.Z. Chen, L. Song, Y.P. Gao, A.P. Zhu, D.L. Cao, Experimental determination of solubilities and supersolubilities of 2, 2', 4, 4', 6, 6'-hexanitrostilbene in different organic solvents, *Chin. J. Chem. Eng.* 25 (6) (2017) 809–814.
[18] I.M. Smallwood, Handbook of Organic Solvent Properties, Elsevier, Amsterdam, 1996.
[19] Y. Wang, T. Luo, J. Chu, G. Liu, Measurement and correlation of solubilities of 1,6-hexanediamine, *Chem. Intermed.* 4 (2008) 54–56.
[20] L.Z. Chen, L. Song, G.C. Lan, J.L. Wang, Solubility and metastable zone width measurement of 3, 4-bis(3-nitrofurazan-4-yl)furoxan (DNTF) in ethanol + water, *Chin. J. Chem. Eng.* 25 (5) (2017) 646–651.
[21] Y.Z. Liu, Y. Xiao, C. Li, L.Z. Chen, Q. Liu, J.L. Wang, Measurement, correlation of solubility and thermodynamic properties of 1, 3-dichloro-2, 4, 6-trinitrobenzene in different mono-solvents, *J. Chem. Thermodyn.* 172 (2022) 106819.
[22] C. Huang, Z.P. Xie, J.C. Xu, Y.J. Qin, Y.N. Du, S.C. Du, J.B. Gong, Experimental and modeling studies on the solubility of d-pantolactone in four pure solvents and ethanol–water mixtures, *J. Chem. Eng. Data* 60 (3) (2015) 870–875.
[23] X.H. Zhao, J.L. Wang, L.Z. Chen, L.Y. Liu, Z.H. Han, C. Zhou, Crystallization thermodynamics of FOX-7 in three binary mixed solvents, *J. Mol. Liq.* 295 (2019) 111445.
[24] A. Apelblat, E. Manzurola, Solubility of oxalic, malonic, succinic, adipic, maleic, malic, citric, and tartaric acids in water from 278.15 to 338.15 K, *J. Chem. Thermodyn.* 19 (3) (1987) 317–320.
[25] A. Apelblat, E. Manzurola, Solubilities ofo-acetylsalicylic, 4-aminosalicylic, 3, 5-dinitrosalicylic, andp-toluic acid, and magnesium-DL-aspartate in water from *T* = (278 to 348) K, *J. Chem. Thermodyn.* 31 (1) (1999) 85–91.
[26] S.S. Li, Y. Liu, F. Yin, X.Y. Ye, Solubility measurement and modeling of 2-amino-4, 6-dichoropyrimidine in ten pure solvents and (ethyl acetate + ethanol) solvent mixtures, *J. Chem. Eng. Data* 63 (10) (2018) 3715–3726.
[27] M. Zheng, J. Chen, G.Q. Chen, R.J. Xu, H.K. Zhao, Solubility modeling and solvent effects of allopurinol in 15 neat solvents, *J. Chem. Eng. Data* 63 (9) (2018) 3551–3558.
[28] H. Renon, J.M. Prausnitz, Local compositions in thermodynamic excess functions for liquid mixtures, *AIChE J.* 14 (1) (1968) 135–144.
[29] A.S. Gow, Calculation of vapor-liquid equilibria from infinite-dilution excess enthalpy data using the Wilson or NRTL equation, *Ind. Eng. Chem. Res.* 32 (12) (1993) 3150–3161.
[30] M. Xue, D.Z. Huang, K.X. Yang, L.Z. Chen, Z.H. Zheng, Y. Xiang, Q.W. Huang, J.L. Wang, Measurement, correlation of solubility and thermodynamic properties analysis of 2, 4, 6-trinitroresorcinol hydrate in pure and binary solvents, *J. Mol. Liq.* 330 (2021) 115639.
[31] M.J. Kamlet, R.M. Doherty, J.L. Abboud, M.H. Abraham, R.W. Taft, Linear solvation energy relationships: 36. Molecular properties governing solubilities of organic nonelectrolytes in water, *J. Pharm. Sci.* 75 (4) (1986) 338–349.
[32] W. Huang, H.R. Wang, C.R. Li, T. Wen, J.K. Xu, J.B. Ouyang, C.T. Zhang, Measurement and correlation of solubility, Hansen solubility parameters and thermodynamic behavior of Clozapine in eleven mono-solvents, *J. Mol. Liq.* 333 (2021) 115894.
[33] Z.B. Huang, Y.Y. Zun, Y. Gong, X.R. Hu, J. Sha, Y. Li, T. Li, B.Z. Ren, Solid-liquid equilibrium solubility, thermodynamic properties, solvent effect of Ipriflavone in twelve pure solvents at various temperatures, *J. Chem. Thermodyn.* 150 (2020) 106231.
[34] Y. Marcus, The properties of organic liquids that are relevant to their use as solvating solvents, *Chem. Soc. Rev.* 22 (6) (1993) 409.
[35] C.M. Hansen, Hansen Solubility Parameters: A User's Handbook, Second Edition., CRC Press, Boca Raton, FL, USA, 2007.
[36] R.R. Krug, W.G. Hunter, R.A. Grieger, Enthalpy-entropy compensation. 1. Some fundamental statistical problems associated with the analysis of van't Hoff and Arrhenius data, *J. Phys. Chem.* 80 (21) (1976) 2335–2341.
[37] J.B. Chaires, Possible origin of differences between van't Hoff and calorimetric enthalpy estimates, *Biophys. Chem.* 64 (1–3) (1997) 15–23.
[38] X.H. Zhao, G.Y. Zhang, D.L. Zhang, L.Z. Chen, J.L. Wang, Solubility and thermodynamic properties of FOX-7 in four binary mixed solvents from *T* = 298.15 to 333.15 K, *J. Mol. Liq.* 322 (2021) 114876.
[39] W.E. Acree Jr, A.I. Zvaigzne, Thermodynamic properties of non-electrolyte solutions, *Thermochim. Acta* 178 (1991) 151–167.
[40] G.L. Perlovich, S.V. Kurkov, A.N. Kinchin, A. Bauer-Brandl, Thermodynamics of solutions III: comparison of the solvation of (+)-naproxen with other NSAIDs, *Eur. J. Pharm. Biopharm.* 57 (2) (2004) 411–420.
[41] Y.H. Hu, X. Liu, W.G. Yang, J.J. Yin, Y. Liu, M.M. Liang, Measurement and correlation of the solubility of 4-methylbenzoic acid in (methanol + acetic acid) binary solvent mixtures, *J. Mol. Liq.* 193 (2014) 213–219.
[42] M. Gantiva, F. Martínez, Thermodynamic analysis of the solubility of ketoprofen in some propylene glycol + water cosolvent mixtures, *Fluid Phase Equilib.* 293 (2) (2010) 242–250.